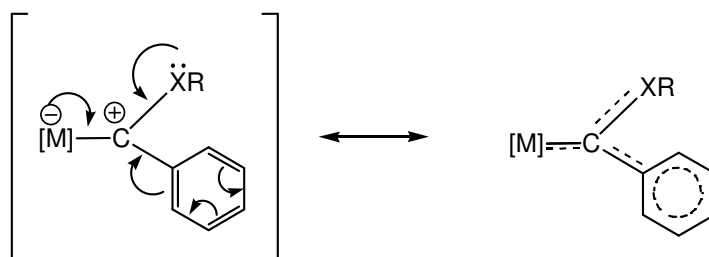


# 2 Dimanganese Monocarbene Complexes

## 2.1 Background

### 2.1.1 Fischer carbene complexes with aromatic substituents

The first reported metal carbene complex  $[W(CO)_5C(OMe)Ph]$  prepared by Fischer and Maasböl<sup>[1]</sup> contained an aromatic substituent phenyl ring. The structural data of the complexes  $[W(CO)_5C(OMe)Ph]$  and  $[Cr(CO)_5C(OMe)Ph]$ <sup>[2]</sup> were published shortly thereafter and showed the  $sp^2$ -character of the carbene carbon atom. The role of the heteroatom (X) lone-pair in  $p_c-p_x$   $\pi$ -bonding to stabilize the "singlet" carbene carbon was recognized<sup>[3;4]</sup> as well as the transition metals' synergic  $d(t_{2g})-p$   $\pi$ -interaction with the carbene carbon atom.



**Figure 2.1**  $\pi$ -delocalized network around carbene carbon atom

A phenyl or heteroarene substituent is incorporated into the  $\pi$ -delocalized network surrounding the carbene carbon atom and can act as either an electron withdrawing or electron donating substituent. Casey and Burkhardt<sup>[5]</sup> then synthesized the stable  $[\text{W}(\text{CO})_5\text{C}(\text{Ph})\text{Ph}]$  carbene complex from  $[\text{W}(\text{CO})_5\text{C}(\text{OEt})\text{Ph}]$  where the phenyl substituent donates electron density.

### 2.1.2 Carbene complexes with heteroaromatic substituents

The first monocarbene complexes of chromium with heteroaromatic substituents were synthesized by Connor and Jones<sup>[6]</sup> (Figure 2.2) in order to study the extent to which the heteroatom Y influences the donating of electron-density to the empty carbene carbon  $p$ -orbital. It was found that the electron-donation of the heteroaromatic ring increases in the order  $\text{Y} = \text{O} < \text{S} < \text{NMe}$ . It can be concluded that N-methylpyrrole will stabilize the carbene carbon the most, leading to less back bonding from the metal to the carbene carbon atom.

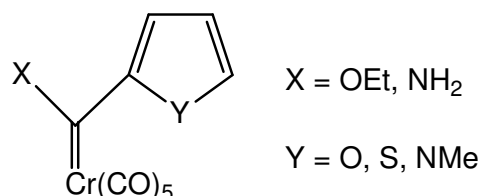


**Figure 2.2** Chromium monocarbene complexes with heteroarene substituents

Since these initial discoveries many examples of carbene complexes of arenes and heterocycles have been reported and these compounds have proven to be useful precursors in catalysis<sup>[7]</sup>. Monocarbene complexes with 2,2'-bithiophene substituents have also been reported<sup>[8]</sup> with the purpose of developing carbene complexes with non-linear optical properties. The general structural motif employing heteroaromatic compounds as conjugated spacer units in mono- and

biscarbene complexes has also been investigated recently in our laboratories<sup>[9-12]</sup>. This was done in aid of the design of complexes specifically tailored for electronic transfer processes within the molecule, and to study regioselective reactions.

### 2.1.3 Binuclear carbene complexes

To determine whether binuclear metal carbonyl complexes can accommodate carbene ligands, Fischer and Offhaus<sup>[13]</sup> successfully synthesized the binuclear  $[\text{Mn}_2(\text{CO})_9\text{C}(\text{OEt})\text{Ph}]$  and  $[\text{Mn}_2(\text{CO})_9\text{C}(\text{OEt})\text{Me}]$  complexes. From the IR spectrum, eight bands were observed for  $[\text{Mn}_2(\text{CO})_9\text{C}(\text{OEt})\text{Me}]$ , corresponding to the  $C_s$  symmetry of an *eq*- $[\text{Mn}_2(\text{CO})_9\text{L}]$  complex. However, for  $[\text{Mn}_2(\text{CO})_9\text{C}(\text{OEt})\text{Ph}]$ , five  $\nu_{\text{CO}}$  bands, corresponding to  $C_{4v}$  symmetry of *ax*- $[\text{Mn}_2(\text{CO})_9\text{L}]$  were seen in the IR spectrum. Shortly after this, Huttner and Regler<sup>[14]</sup> reported the crystal structure of  $[\text{Mn}_2(\text{CO})_9\text{C}(\text{OEt})\text{Ph}]$ , and found the carbene ligand to be in the equatorial position ( $C_s$ ), and the Et in the *cis* configuration with respect to the C-O bond, in contrast to the *trans* configuration found in the X-ray crystal structure of  $[\text{Cr}(\text{CO})_5\{\text{C}(\text{OMe})(\text{Ph})\}]$ <sup>[14]</sup>. This was ascribed to the fact that an equatorially substituted carbene ligand would be too sterically hindered to accommodate the substituents on the carbene ligand in the *trans* configuration, and they explained the appearance of five IR bands instead of eight, as a result of degeneracy and band overlap.

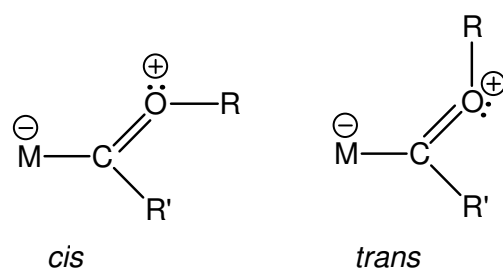
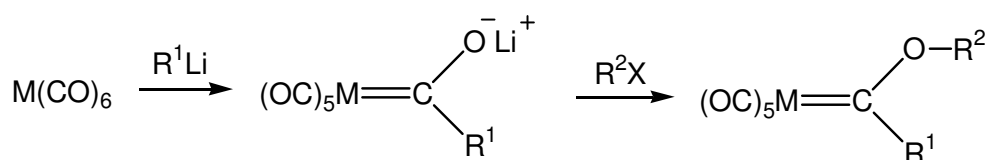


**Figure 2.3** *Cis* and *trans* configurations around C-O bond

## 2.1.4 Preparatory methods

To synthesize alkoxy carbene complexes, the most general route is the addition of an organolithium reagent to a metal carbonyl to give an acyl metallate, which undergoes O-alkylation by strong alkylating reagents such as trialkyloxonium salts, alkyl fluorosulfonates or alkyl trifluoromethanesulfonates. This classical Fischer route<sup>[1]</sup> to metal carbene complexes is given in Scheme 2.1. Another widely used alternative approach was developed by Hegedus and Semmelhack<sup>[15;16]</sup> (Scheme 2.2) whereby an organoelectrophile is combined with a metal nucleophile.



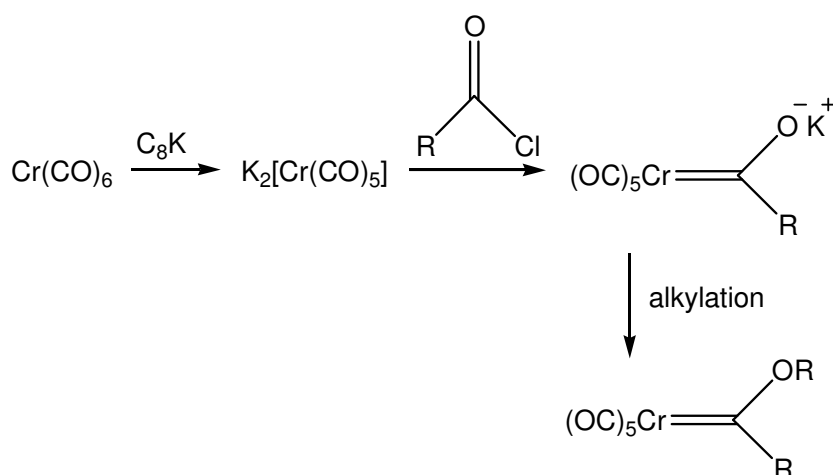
M = Cr, Mo, W

R<sup>1</sup> = alkyl, aryl, vinyl

R<sup>2</sup>X = R<sup>2</sup><sub>3</sub>O<sup>+</sup>BF<sub>4</sub><sup>-</sup>, R<sup>2</sup>OSO<sub>2</sub>F

R<sup>2</sup> = Et, Me

**Scheme 2.1** Fischer synthesis of metal carbene complexes



**Scheme 2.2** Hegedus-Semmelhack synthesis of alkoxy carbene complexes

$C_8K$  was found to be an efficient reducing agent to convert  $Cr(CO)_6$  to  $K_2[Cr(CO)_5]$ .

For Group VII transition metals, carbene complexes with cyclopentadienyl ligands are readily accessible from  $MCp(CO)_3$  and organolithium reagents<sup>[17;18]</sup>, while binuclear monocarbene complexes can be obtained from  $M_2(CO)_{10}$  and organolithium precursors<sup>[13;19;20]</sup>. Binuclear monocarbene complexes of manganese were also prepared by the reaction of  $Na[Mn(CO)_5]$  and dihaloalkanes or acetyl halides<sup>[21-23]</sup>, similar to the method employed by Hegedus and Semmelhack (Scheme 2.2).

### 2.1.5 Focus of this study

The synthesis of novel dinuclear monocarbene complexes of the Group VII transition metal, manganese, containing a range of heteroarene substituents (2,2'-bithiophene, thiophene, furan and N-methylpyrrole) was planned as the first step in this study. The furyl-substituted dirhenium monocarbene was also synthesized in this chapter for comparison with its manganese analogue, to study steric and electronic properties of the carbene ligand in binuclear complexes. Figure 2.4 is a representation of the five complexes synthesized in this chapter.

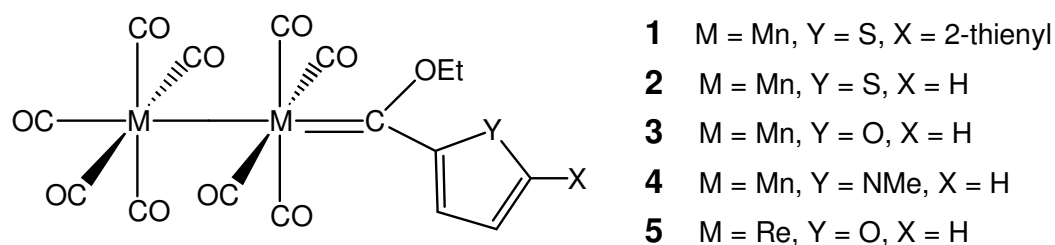
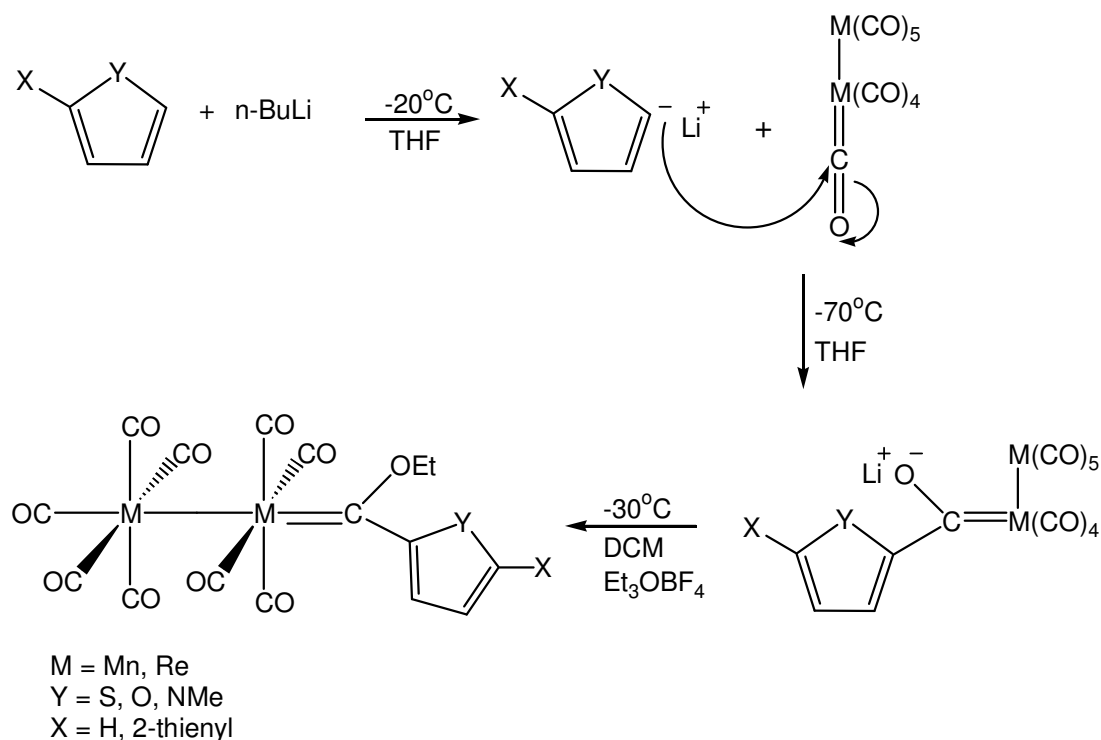


**Figure 2.4** Dinuclear monocarbene complexes of manganese and rhenium

## 2.2 Synthesis

Fischer's classical approach was utilised in the syntheses of the desired binuclear monocarbene complexes  $[M_2(CO)_9(\text{carbene})]$  ( $M = \text{Mn, Re}$ ) (Scheme 2.3).



**Scheme 2.3** Syntheses of Complexes 1 - 5

Deprotonation of the acidic  $\alpha$ -proton of the heteroarenes is accomplished by the use of the strong base  $n\text{-BuLi}$  in THF at  $-20^\circ\text{C}$ . After addition of the bimetallic decacarbonyl to the reaction mixture at  $-70^\circ\text{C}$ , the resulting nucleophilic  $\alpha$ -carbon of the heteroarene ring attacks an electron-deficient carbon of the bimetal decacarbonyl to form a metal acylate. After removing the THF under reduced pressure, the residue is dissolved in dichloromethane. Alkylation is then carried out by adding triethyloxonium salt to the metal acylate at  $-30^\circ\text{C}$  and purification of the product to remove unreacted metal decacarbonyl is achieved by column chromatography. The desired neutral carbene complexes are formed in yields ranging from 63 - 74%. The monocarbene complexes **2**, **3** and **5** were

crystallized from a hexane:dichloromethane (1:1) solution and afforded orange-red crystals. Complexes **1** and **4** were isolated and characterized spectroscopically, but no high quality crystals could be obtained.

## **2.3 Characterisation**

The binuclear monocarbene complexes **1** - **5** were characterized in solution using NMR and infrared spectroscopy, as well as FAB mass spectrometry and in the solid state by molecular crystal structure determinations.

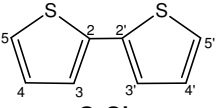
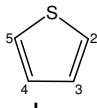
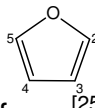
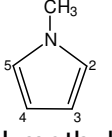
### **2.3.1 NMR Spectroscopy**

#### **2.3.1.1 <sup>1</sup>H NMR Spectroscopy**

The chemical shifts in the <sup>1</sup>H NMR spectrum of the uncoordinated heteroarene rings are given in Table 2.1. The assignment of the chemical shifts of the protons of these uncoordinated ligands was based on the assignments made by the references given in the table for each heteroarene.

The NMR spectra of complexes **1**, **4** and **5** were recorded in deuterated chloroform as solvent but spectra of high resolution could only be obtained for complexes **2** and **3** in d<sub>6</sub>-acetone. Slow decomposition of products with time was observed in the spectra, and broadening of the signals in the case of the N-methyl pyrrole-substituted carbene complex **4**. Chemical shifts are given in Table 2.2.

**Table 2.1**  $^1\text{H}$  NMR data of uncoordinated heteroarenes

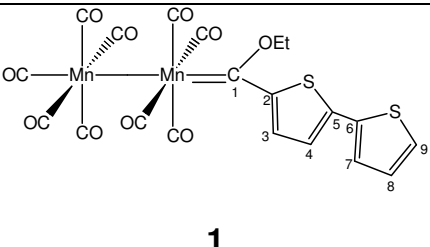
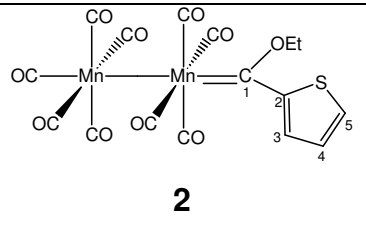
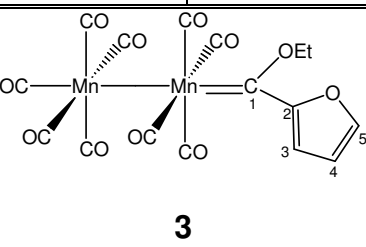
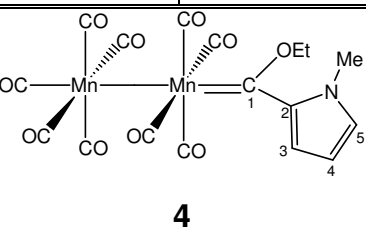
Assignment	 2,2'- bithiophene <sup>[11]</sup>	Assignment	 thiophene <sup>[24]</sup>	 furan <sup>[25]</sup>	 N-methyl pyrrole <sup>[26]</sup>
Proton	Chemical shift ( $\delta$ , ppm)	Proton	Chemical shift ( $\delta$ , ppm)		
H3, H3'	7.18	H2, H5	7.20	7.38	6.60
H4, H4'	7.02	H3, H4	6.96	6.30	6.13
H5, H5'	7.21	N-CH <sub>3</sub>	-	-	3.66

On comparing the literature chemical shift values of the uncoordinated heteroarenes with the corresponding values of the complexes, it is clear that the coordination to a metal fragment has a marked influence on the chemical shifts of the protons. Upon coordination to the metal, the carbene moiety causes draining of electron density from the double bonds of the heteroarene ring to the electrophilic carbene moiety, resulting in a downfield shift of the protons of the coordinated rings compared to the uncoordinated heteroarenes. Assignments of the ring protons of the 2,2'-bithienyl, thienyl and N-methyl pyrrolyl substituents are based on the assignments made by Gronowitz<sup>[27]</sup>.

The more downfield shifts of H3 and H5 compared to H4 can be explained by considering the resonance structures of the complexes as shown in Figure 2.5. Deshielding of protons H3 and H5 are effected by the positive charges afforded on these two protons caused by the  $\pi$ -resonance effect. Proton H4 is not affected by the resonance effect and therefore its chemical shift is comparable to that of the free heteroarene.



**Table 2.2**  $^1\text{H}$  NMR data of complexes **1** - **5**

Assignment	Complexes			
	Chemical shifts ( $\delta$ , ppm) and coupling constants ( $J$ , Hz)			
	 <b>1</b>		 <b>2</b>	
Proton	$\delta^a$	$J$	$\delta^b$	$J$
H3	8.33 (d)	4.4	8.35 (dd)	4.1, 0.8
H4	7.61 (d)	4.4	7.42 (dd)	4.9, 4.1
H5	-	-	8.07 (dd)	5.0, 0.8
H7	7.65 (dd)	3.6, 0.8	-	-
H8	7.23 (dd)	5.0, 3.6	-	-
H9	7.76 (dd)	4.1, 0.8	-	-
-OCH <sub>2</sub> CH <sub>3</sub>	5.31 (q)	7.0	5.32 (q)	7.0
-OCH <sub>2</sub> CH <sub>3</sub>	1.79 (t)	7.0	1.80 (t)	7.0
Assignment	 <b>3</b>		 <b>4</b>	
Proton	$\delta^b$	$J$	$\delta^a$	$J$
H3	7.19 (dd)	3.9, 1.9	7.90	-
H4	6.85 (dd)	3.9, 0.7	6.58	-
H5	7.46 (dd)	3.9, 0.7	7.40	-
-OCH <sub>2</sub> CH <sub>3</sub>	5.28 (q)	7.0	5.25 (q)	7.0
-OCH <sub>2</sub> CH <sub>3</sub>	1.76 (t)	7.0	1.81 (t)	7.0
-NCH <sub>3</sub>	-	-	3.93 (s)	-

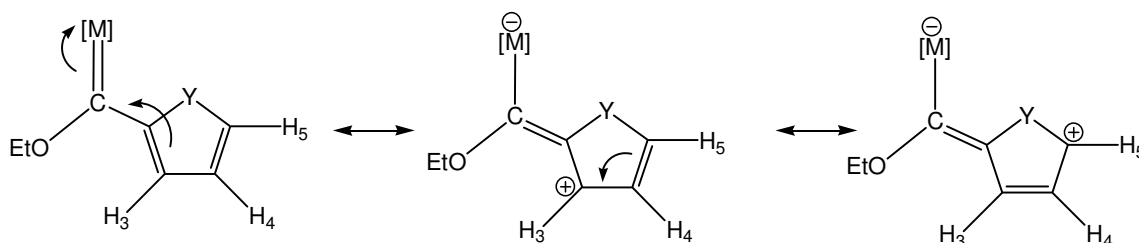
 a) Spectra recorded in CDCl<sub>3</sub>    b) Spectra recorded in acetone-d<sub>6</sub>

**Table 2.2 contd.** <sup>1</sup>H NMR data of complex **5**

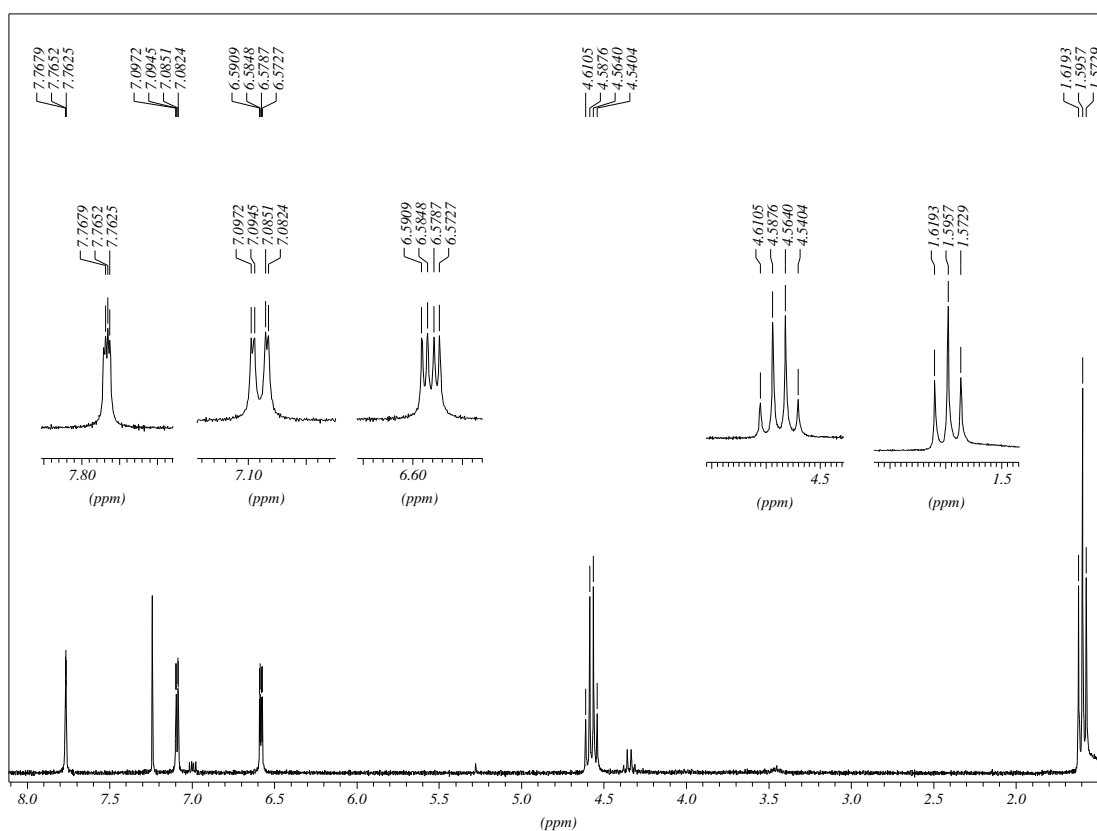
Assignment	Complex	
	Chemical shifts ( $\delta$ , ppm) and coupling constants ( $J$ , Hz)	
	 <b>5</b>	
Proton	$\delta^a$	$J$
H3	7.09 (dd)	3.6, 0.8
H4	6.58 (dd)	3.6, 1.8
H5	7.77 (dd)	1.6, 0.8
-OCH <sub>2</sub> CH <sub>3</sub>	4.58 (q)	7.0
-OCH <sub>2</sub> CH <sub>3</sub>	1.60 (t)	7.0

 a) Spectra recorded in CDCl<sub>3</sub>

The atypical assignment of the furyl ring proton chemical shifts of complexes **3** and **5** is based on the assignments made by Crause<sup>[11]</sup> for chromium complexes, which agrees well with the predicted shifts for an ester derivative<sup>[25]</sup>.


**Figure 2.5**  $\pi$ -resonance effect in monocarbene complex

The heteroarene resonances, the methylene quartet and the methyl triplet of the ethoxy group, with relative intensities of 1:2:3, were clearly evident in all spectra (Figure 2.6). The large downfield shift of the methylene protons of the ethoxy-group is consistent with the strong electron withdrawing character of the  $M(\text{CO})_5\{\text{C}(\text{C}_4\text{H}_3\text{Y})\}$  ( $\text{Y} = \text{S}, \text{O}, \text{N-Me}$ ) groups, compared to the signal of approximately 3.6 ppm observed for normal  $-\text{CH}_2\text{OR}$  protons. The chemical shifts of these methylene protons are characteristic for a specific metal, as shown by the difference in methylene, methyl chemical shifts for complex **3** (5.28 ppm, 1.76 ppm) and complex **5** (4.58 ppm, 1.60 ppm), the 2-furyl substituted dimanganese and dirhenium carbene complexes, respectively, and insensitive to the number and type of carbene substituents (compare complexes **1 - 4**). On the other hand, the number of carbene ligands as well as the nature of the transition metal involved determines the chemical shifts of the ring protons of the heterocycle.

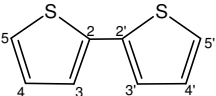
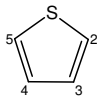
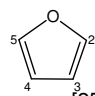
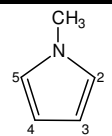


**Figure 2.6**  $^1\text{H}$  NMR spectrum of complex **5** in  $\text{CDCl}_3$ , with expansion of ring and methylene proton signals

### 2.3.1.2 $^{13}\text{C}$ NMR Spectroscopy

The chemical shifts in the  $^{13}\text{C}$  NMR spectra for the free heterocycles are known from literature<sup>[11;24-26]</sup> and are given in Table 2.3. The  $^{13}\text{C}$  NMR data for the binuclear monocarbene complexes **1** - **3** and **5** are summarized in Table 2.4, although no  $^{13}\text{C}$  NMR data could be obtained for **4**, as this complex decomposed during data collection. The chemical shift assignments (C3 - C9) of the 2,2'-bithienyl monocarbene complex are based on the assignments made and corroborated by 2D HETCOR NMR spectra for chromium and tungsten carbene complexes synthesized by Crause<sup>[11]</sup>.

**Table 2.3**  $^{13}\text{C}$  NMR data of uncoordinated heteroarenes

Assignment	 2,2'- bithiophene <sup>[11]</sup>	Assignment	 thiophene <sup>[24]</sup>	 furan <sup>[25]</sup>	 N-methyl pyrrole <sup>[26]</sup>
Carbon	Chemical shift ( $\delta$ , ppm)	Carbon	Chemical shift ( $\delta$ , ppm)		
C2, C2'	137.4	C2, C5	127.6	143.0	124.3
C3, C3'	123.7	C3, C4	125.8	109.9	111.2
C4, C4'	127.7	N-CH <sub>3</sub>	-	-	38.1
C5, C5'	124.3	-	-	-	-

Fischer carbene carbon atoms are defined as being electron-deficient  $sp^2$ -hybridized carbons stabilized by dative  $\pi$ -bonding from the heteroatom in the alkoxy substituent and from the metal combined with inductive release from the heteroaromatic substituent. Spectroscopic data supports this model as metal carbene carbon shifts can be found very downfield in a broad range of 200<sup>[28]</sup> to 400<sup>[29]</sup> ppm and the chemical shift of the carbene ligands decrease as a function of the donor properties of the heterocyclic substituent<sup>[6]</sup> as follows:

2,2'-bithienyl > 2-thienyl > 2-furyl. This trend was observed on comparing the spectra of complexes **1**, **2** and **3**.

The carbene carbon resonances depend both on the carbene substituents and on the metal, and are more sensitive to changes in the electronic environment than the carbonyl ligands.

**Table 2.4**  $^{13}\text{C}$  NMR data of complexes **1** - **5** recorded in  $\text{CDCl}_3$

Assignment	Complexes			
	<b>1</b>	<b>2</b>	<b>3</b>	<b>5</b>
Carbon*	$\delta$ (ppm)	$\delta$ (ppm)	$\delta$ (ppm)	$\delta$ (ppm)
C1	309.9	306.5	301.0	283.2
C2	162.1	155.4	163.9	165.5
C3	140.9	133.9	112.8	114.7
C4	125.3	128.9	110.1	113.9
C5	146.8	138.9	149.5	151.6
C6	134.4	-	-	-
C7	127.8	-	-	-
C8	128.8	-	-	-
C9	126.6	-	-	-
$\text{M}(\text{CO})_4$	222.7	224.6	223.9	193.9
$\text{M}(\text{CO})_5$	211.0, n.o.	221.0, 208.9	219.5, 221.4	190.4, 188.5
$-\text{OCH}_2\text{CH}_3$	74.4	74.6	74.2	77.6
$-\text{OCH}_2\text{CH}_3$	15.5	15.1	15.1	14.7

\* See Table 2.2 for numbering of carbons

Chemical shifts for terminal metal carbonyls lie in the range of 150 to 240 ppm<sup>[30]</sup> with shielding of the carbonyl nucleus increasing with increasing atomic number of the metal, as shown by the carbonyl resonances of complex **3** (223.9, 221.4 and 219.5 ppm), the manganese analogue of the dirhenium complex **5** (193.9, 190.4 and 188.5 ppm). On the other hand, the carbonyl groups are fairly insensitive to changes of substituents on ligands, e.g. replacing a 2,2'-bithienyl substituent with either a 2-thienyl or a 2-furyl substituent. Three carbonyl signals are observed in each spectrum. The most downfield shift can be assigned to the

M(CO)<sub>4</sub>-fragment, while the other two signals can be attributed to the *cis* and *trans* carbonyl ligands of the M(CO)<sub>5</sub>-fragment.

As in the case of the <sup>1</sup>H NMR spectra, slow decomposition of the complexes were observed in the <sup>13</sup>C NMR spectra, as indicated by the repetition of the heteroarene signals. The decomposition products could be the ester analogues<sup>[31]</sup> of the carbene complexes, although no further investigation into these decomposition products were carried out.

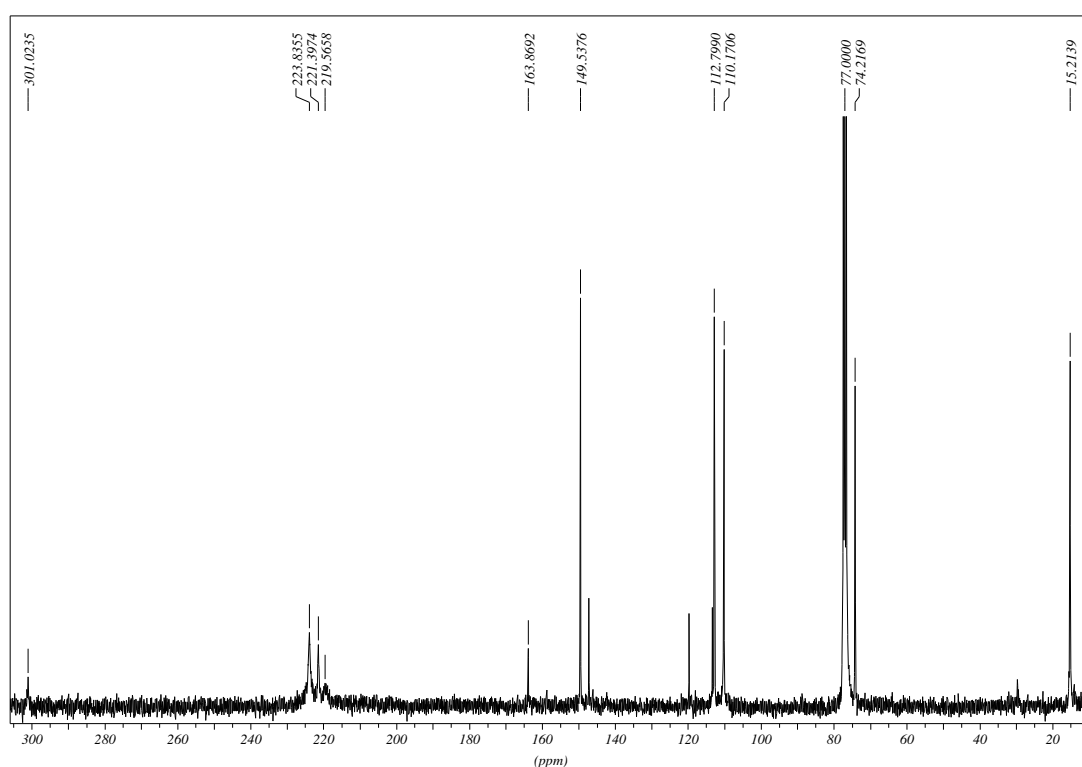


**Figure 2.7** <sup>13</sup>C NMR spectrum of complex **3**

### 2.3.2 IR Spectroscopy

The stretching vibrational frequency of a free CO group is 2143 cm<sup>-1</sup>, but lies between 1850 and 2120 cm<sup>-1</sup> for terminal carbonyl ligands<sup>[32]</sup>. In contrast to M-C stretching frequencies, the C-O stretching vibrational frequencies can be seen as being independent from other vibrations in the molecule, thus a qualitative

correlation between CO stretching vibrational frequencies and the bond order of the C-O bond can be made.

As backbonding from the metal to the carbonyl ligand increases, the M-C bond becomes stronger and thus shorter. The C-O bond weakens accordingly and becomes longer, and the carbonyl stretching frequency shifts to a lower wave number on the IR spectrum. Carbene ligands have weaker  $\pi$ -acceptor properties compared to carbonyl groups, which means back bonding from the metal to the carbonyl ligand increases. This is shown by the lower wave numbers of the bands caused by  $\nu_{\text{CO}}$  vibrations in carbene carbonyl complexes compared to the corresponding metal carbonyl complexes.

The number and intensities of carbonyl stretching frequencies are dependent on the local symmetry of the carbonyl ligands around the central atom. The carbonyl stretching modes of equatorially and axially substituted bimetal nonacarbonyl complexes were summarized by Ziegler *et al*<sup>[33]</sup>. The *eq*-[M<sub>2</sub>(CO)<sub>9</sub>L] displays a nine band pattern in the IR spectrum, corresponding to C<sub>s</sub> symmetry (Figure 2.8). These bands include six A' bands and three degenerate A'' bands. On the other hand, the IR spectrum of *ax*-[M<sub>2</sub>(CO)<sub>9</sub>L] is observed to have only five bands: the three A' bands and two E bands which corresponds with C<sub>4v</sub> symmetry (Figure 2.9).

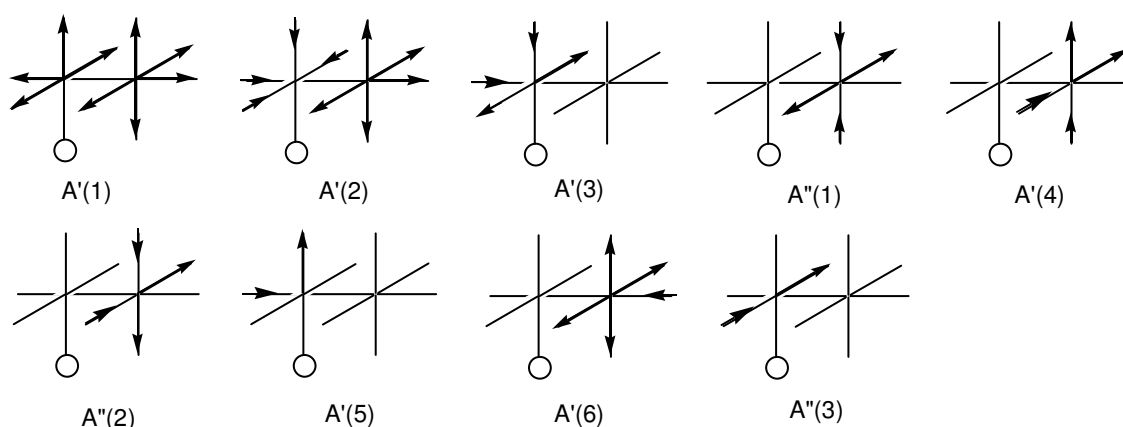


**Figure 2.8** IR-active normal modes observed for *eq*-[M<sub>2</sub>(CO)<sub>9</sub>L]

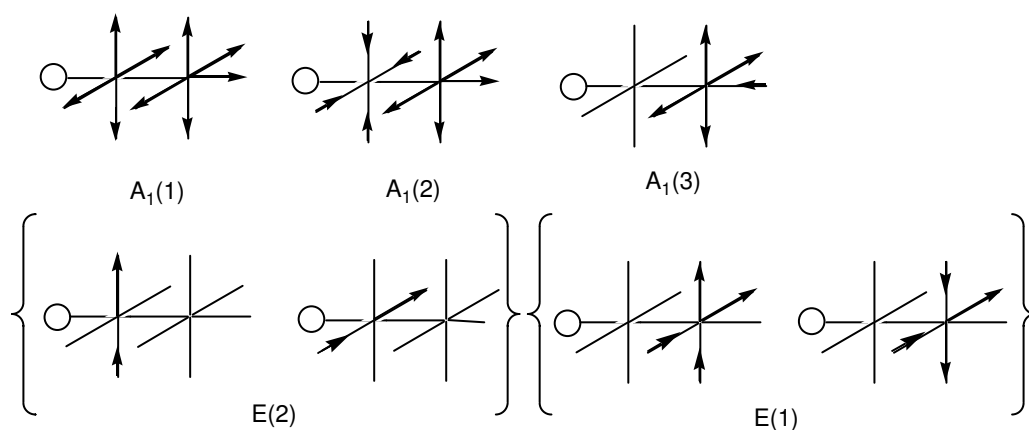


**Figure 2.9** IR-active normal modes observed for  $ax-[M_2(CO)_9L]$

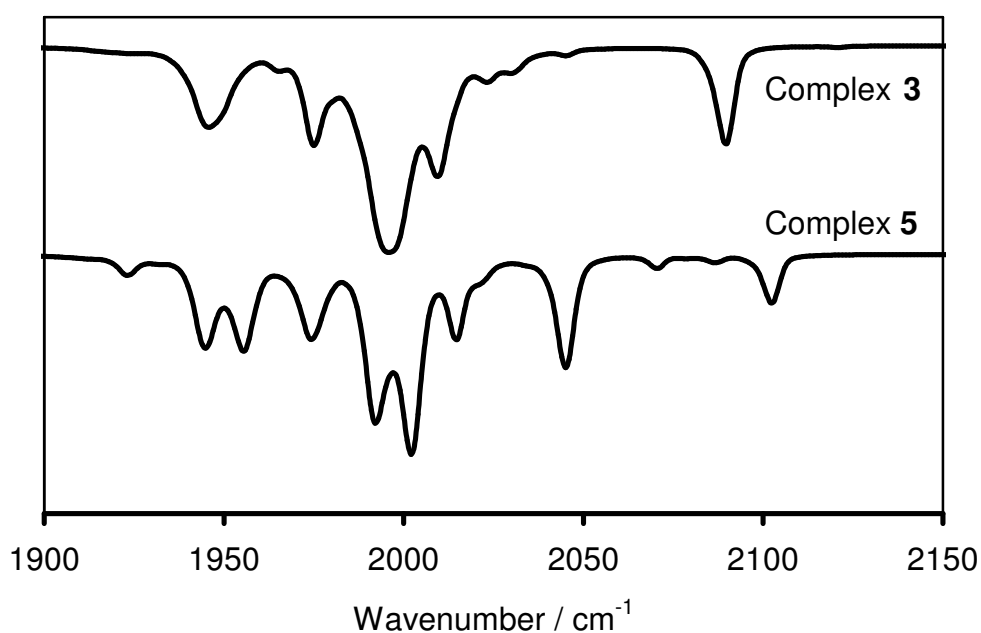


**Figure 2.10** Stacked IR spectra of complexes **3** and **5** in the carbonyl region

The  $[Re_2(CO)_9\{C(OEt)(2-furyl)\}]$  complex **5** displayed the expected typical nine band pattern for an equatorially substituted bimetal nonacarbonyl complex with  $C_s$  symmetry<sup>[33]</sup> (Table 2.6, Figure 2.10). However, the IR spectra of all the dimanganese monocarbene complexes **1** - **4** displayed only five carbonyl stretching bands in the carbonyl region (Table 2.5, Figure 2.10). This five band



pattern indicates  $C_{4v}$  symmetry, but needs to be examined carefully as the number of bands in  $eq\text{-}[\text{Mn}_2(\text{CO})_9\text{L}]$  may be less than nine because of band overlap.  $C_{4v}$  symmetry places the carbene ligand in an axial position relative to the Mn-Mn bond. A search of the Cambridge Structural Database revealed that only one other axially substituted carbene complex of dimanganese nonacarbonyl has been structurally characterized. This complex has the unusual carbene ligand,  $(\text{M})=\text{C}(\text{NMe}_2)\text{OAl}_2(\text{NMe}_2)_5$ <sup>[34]</sup>.

**Table 2.5** IR data in the carbonyl region of complex **1** - **4**<sup>a</sup>

Complex	Carbonyl stretching frequencies ( $\nu_{\text{CO}}$ , $\text{cm}^{-1}$ ) for pseudo- $C_{4v}$ symmetry of $ax\text{-}[\text{Mn}_2(\text{CO})_9(\text{carbene})]$				
	A <sub>1</sub> (1)	A <sub>1</sub> (2)	E (1)	A <sub>1</sub> (3)	E (2)
<b>1</b>	2089 (m)	2009 (m)	1996 (vs)	1975 (m)	1945 (m)
<b>2</b>	2090 (m)	2010 (m)	1996 (vs)	1975 (m)	1946 (m)
<b>3</b>	2087 (m)	2006 (m)	1992 (vs)	1971 (m)	1936 (m)
<b>4</b>	2089 (m)	2009 (m)	1996 (vs)	1975 (m)	1944 (m)

a) Hexane as solvent

**Table 2.6** IR data in the carbonyl region of complex **5**<sup>a</sup>

Complex	Carbonyl stretching frequencies ( $\nu_{\text{CO}}$ , $\text{cm}^{-1}$ ) for $C_s$ - symmetry of $eq\text{-}[\text{Re}_2(\text{CO})_9(\text{carbene})]$								
	A'(1)	A'(2)	A'(3)	A''(1)	A'(4)	A''(2)	A'(5)	A'(6)	A''(3)
<b>5</b>	2102 (w)	2045 (m)	2016 (s)	2002 (vs)	1992 (s)	1974 (m)	1955 (m)	1945 (m)	1923 (w)

a) Hexane as solvent

### 2.3.3 Mass Spectrometry

A molecular ion peak,  $M^+$ , was observed in the mass spectra for complexes **1**, **2**, **3** and **5**, although with a low intensity.

**Table 2.7** Mass spectral data of binuclear monocarbene complexes

Complex	m/z	Intensity (%)	Fragment ion
<b>1</b>	584	7	$[M]^+$
	556	4	$[M - CO]^+$
	511	12	$[M - CO - OEt]^+$
	500	4	$[M - 3CO]^+$
	472	13	$[M - 4CO]^+$
	195	9	$[Mn(CO)_5]^+$
<b>2</b>	502	2	$[M]^+$
	390	15	$[M - 4CO]^+$
	279	2	$[M - Mn - 6CO]^+$
<b>3</b>	486	9	$[M]^+$
	413	8	$[M - CO - OEt]^+$
	374	7	$[M - 4CO]^+$
	263	35	$[M - Mn - 6CO]^+$
	235	45	$[M - Mn - 7CO]^+$
	207	30	$[M - Mn - 8CO]^+$
<b>5</b>	749	28	$[M]^+$
	721	5	$[M - CO]^+$
	681	5	$[M - (2-furyl)]^+$
	423	19	$[M - Re - 5CO]^+$

The identified fragment ions ( $m/z$ ) are summarized in Table 2.7. The general initial fragmentation pattern in which the carbonyl ligands were lost sequentially, followed by the loss of an ethyl/methyl group and carbene ligand were observed, although not as consistently as reported by Crause<sup>[11]</sup> and Landman<sup>[12]</sup> for

monocarbene complexes with similar ligands, but with chromium, tungsten and molybdenum metal centres. This fact could be ascribed due to interaction of the compounds with the FAB matrix of nitrobenzyl alcohol.

### 2.3.4 X-Ray Crystallography

Single crystal X-ray diffraction studies confirmed the molecular structure of complexes **2**, **3** and **5**, but no suitable diffraction quality crystals of complex **1** and **4** were obtained. The crystal structures supported the information obtained from the infrared data that the dimanganese monocarbene complexes have an axially substituted carbene ligand while the dirhenium monocarbene has the expected equatorial configuration. The complexes crystallized from a dichloromethane:hexane (1:1) solution by layering of the solvents, yielding orange-red crystals for **2** and **3** and red crystals for **5** of good quality. Figures 2.11, 2.12 and 2.13 represent the ORTEP<sup>[35]</sup> + POV-Ray<sup>[36]</sup> plots of the geometry of the structures **2**, **3** and **5**, and also indicate the atom numbering system used for the structural data.

The crystal structure of free thiophene was determined by Harshbarger and Bauer<sup>[37]</sup> while Liescheski and Rankin<sup>[38]</sup> determined the molecular structure of furan by using various combinations of data from gas-phase electron diffraction, rotational spectroscopy and liquid crystal NMR spectroscopy. The geometrical parameters of these two free heteroarenes are summarized in Table 2.8.

Both complex **2** and **3** crystallized in the monoclinic system, space group  $P2_1/c$  with four molecules in the unit cell. Complex **5** crystallized in the orthorhombic system, space group  $Pbca$  with eight molecules in the unit cell. Selected bond lengths and angles determined for the complexes are tabulated in Table 2.9, whilst the most important torsion angles are listed in Table 2.10. The complete set of crystallographic data of **2**, **3** and **5** are listed in Appendices 1, 2 and 3 respectively.

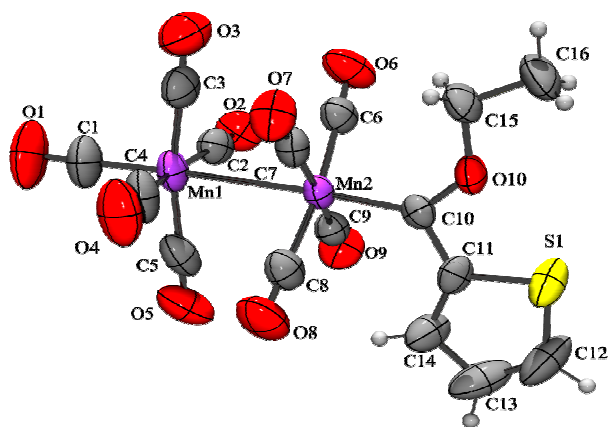


**Figure 2.11** ORTEP + POV-Ray plot of the geometry of complex 2

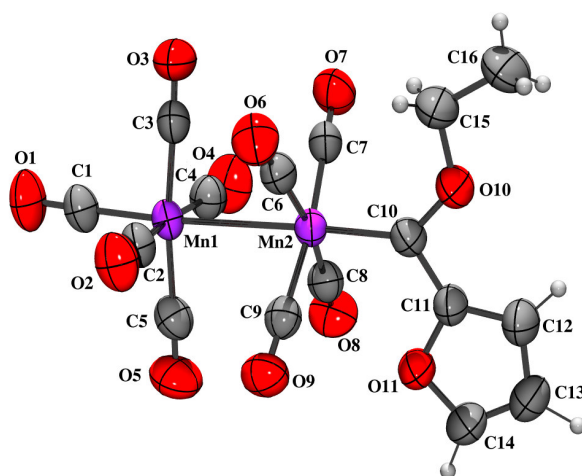


**Figure 2.12** ORTEP + POV-Ray plot of the geometry of complex 3

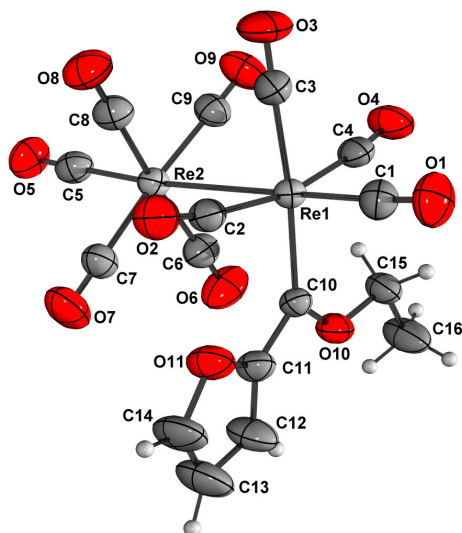


**Figure 2.13** ORTEP + POV-Ray plot of the geometry of complex **5**

**Table 2.8** Geometrical parameters of free thiophene and furan

Thiophene			
Atoms	Bond Lengths (Å)	Atoms	Bond Angles (°)
S-C(2)	1.718(4)	C(2)-S-C(5)	92.0(3)
C(2)-C(3)	1.370(4)	S-C(2)-C(3)	111.2(3)
C(3)-C(4)	1.442(2)	C(2)-C(3)-C(4)	112.5(3)
Furan			
Atoms	Bond Lengths (Å)	Atoms	Bond Angles (°)
O-C(2)	1.3641(7)	C(2)-O-C(5)	106.74(7)
C(2)-C(3)	1.3640(9)	O-C(2)-C(3)	110.49(7)
C(3)-C(4)	1.4303(19)	C(2)-C(3)-C(4)	106.14(6)

For complexes **2** and **3**, the coordination of each manganese atom is approximately octahedral with the two sets of the equatorial carbonyl ligands being staggered. The carbene ligand is in the axial position and is therefore

*trans* to the metal-metal bond. Both the thienyl and the furyl rings are close to being coplanar with the plane of the bonding geometry about the carbene carbon. For **2**, the dihedral angle between the least-squares planes through {S(1), C(11), C(12), C(13) and C(14)} and through {C(10), C(11), O(10) and Mn(2)} is 7.6(9)°. The plane of the carbene carbon, thienyl/furyl ring and oxygen is approximately perpendicular to the equatorial plane of carbonyl ligands {C(10)-Mn(2)-CO (91 - 96°)} and is in an intermediate position between the carbonyl ligands around Mn(2), as is evident from the torsion angles of 45.5(10)° and -44.9(10)° (complex **2**) and -41.0(2)° and 48.7(2)° (complex **3**) for C(6)-Mn(2)-C(10)-O(10) and C(7)-Mn(2)-C(10)-O(10) respectively.

**Table 2.9** Selected bond lengths and angles of **2**, **3** and **5**

Atoms	Bond Lengths (Å)		Atoms	Bond Angles (°)	
	<b>2</b> (Y = S)	<b>3</b> (Y = O)		<b>2</b> (Y = S)	<b>3</b> (Y = O)
Mn(1)-C(1)	1.798(7)	1.813(2)	Mn(2)-C(10)-O(10)	131.1(6)	131.79(16)
Mean Mn(1)-C(x) (x=2,3,4,5)	1.841(9)	1.846(3)	O(10)-C(10)-C(11)	103.8(5)	103.25(18)
Mn(1)-Mn(2)	2.9238 (14)	2.9316(5)	C(11)-C(10)-Mn(2)	125.1(6)	124.96(15)
Mean Mn(2)-C(x) (x=6,7,8,9)	1.833(7)	1.858(2)	C(11)-Y-C(14)	92.3(5)	107.0(2)
Mn(2)-C(10)	1.933(7)	1.932(2)	Y-C(11)-C(12)	109.0(6)	107.4(2)
C(10)-O(10)	1.312(7)	1.332(3)			
C(10)-C(11)	1.470(11)	1.446(3)	Y-C(14)-C(13)	112.3(8)	110.8(3)
C(11)-C(12)	1.384(10)	1.352(3)			
C(12)-C(13)	1.390(12)	1.403(4)	C(12)-C(13)-C(14)	114.0(9)	106.6(2)
C(13)-C(14)	1.313(19)	1.317(4)			
C(11)-Y	1.715(10)	1.379(3)	C(11)-C(12)-C(13)	112.3(9)	108.2(2)

**Table 2.9 contd.** Selected bond lengths and angles of **5**

Atoms	Bond Lengths (Å)	Atoms	Bond Angles (°)
Re(2)-C(5)	1.934(4)	Re(1)-C(10)-O(10)	130.2(3)
Mean Re(2)-C(x) (x=6,7,8,9)	1.989(5)	O(10)-C(10)-C(11)	103.1(3)
Re(1)-Re(2)	3.0809(3)	C(11)-C(10)-Re(1)	126.6(3)
Re(1)-C(1)	1.923(5)		
Re(1)-C(3)	1.992(5)	C(11)-O(11)-C(14)	106.6(4)
Mean Re(1)-C(x) (x=2,4)	1.990(4)		
Re(1)-C(10)	2.129(4)	O(11)-C(11)-C(12)	108.9(4)
C(10)-O(10)	1.323(5)		
C(10)-C(11)	1.457(5)	O(11)-C(14)-C(13)	111.2(4)
C(11)-C(12)	1.355(6)		
C(12)-C(13)	1.418(7)	C(12)-C(13)-C(14)	105.9(5)
C(13)-C(14)	1.331(8)		

Some disorder of the ethoxy-thien-2-yl-methylidene ligand was observed with a minor component rotated approximately 180° about the Mn-C(carbene) bond with respect to the orientation of the major component, such that the C(11)A, C(12)A and C(13)A atoms of the thienyl ring of the minor component nearly coincide with the O(10), C(15) and C(16) atoms, respectively, of the ethoxy group of the major component (O(10)A, C(15)A and C(16)A also nearly coincide with C(11), C(12) and C(13) respectively). This disorder is shown in Figure 2.14. Figure 2.11 shows the major orientation (88.2(4)%).

The carbene ligand is in the *trans*-configuration about the C-O bond (C(11)-C(10)-O(10)-C(15) 177.2(8)° (complex **2**) and -178.9(3)° (complex **3**). The metal-carbon(carbonyl) bond distance *trans* to the Mn-Mn bond is significantly shorter than the mean distance of the Mn-C(carbonyl) bond lengths in the equatorial planes (Table 2.9) to compensate for the weaker  $\pi$ -acceptor properties of the

carbene carbon compared to a carbonyl carbon on the other side of the metal-metal bond.

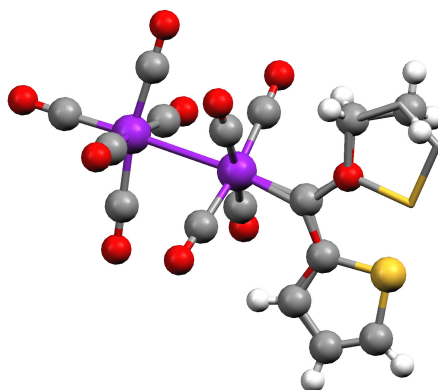


**Figure 2.14** The major (88.3(5)%) and minor (11.7(5)%) orientations of the disordered (C<sub>4</sub>H<sub>3</sub>S)-C-OEt ligand of **2**

The Mn(1)-Mn(2) distance is longer and the *trans* Mn-C(carbonyl) distance is of the same order magnitude when comparing the corresponding Mn-Mn (2.90381(6)Å) and *trans* Mn-C(carbonyl) (1.811(3)Å) distances reported for [Mn<sub>2</sub>(CO)<sub>10</sub>]<sup>[39]</sup>. The Mn-C(carbene), Mn-Mn and M-C(carbonyl) distances are similar in the dimanganese nonacarbonyl carbene complex *eq*-[Mn<sub>2</sub>(CO)<sub>9</sub>{C(OEt)Ph}] where the carbene ligand is in an equatorial position and the carbene substituents are in the *cis*-configuration about the carbene C-O bond. The Mn-C(carbene)-C angles are identical for the axial and equatorial carbene ligands, however, the other bond angles about the carbene carbon are significantly different with Mn-C(carbene)-O 119.4(3)° and C-C(carbene)-O 115.5(3)° in [Mn<sub>2</sub>(CO)<sub>9</sub>{C(OEt)Ph}]<sup>[14]</sup>. The large Mn(2)-C(10)-O(10) angle in **2** and **3** (131.1(6)° and 131.79(16)° respectively) can be ascribed to the steric interactions between the -CH<sub>2</sub> of the ethyl group and the adjacent equatorial carbonyl ligands.

The bond C(11)-C(12) (1.384(10) and 1.352(3) Å for **2** and **3**, respectively) is slightly longer than a double C=C bond, and than the corresponding C(2)-C(3) bonds (1.370(4)Å for thiophene, 1.3640(9)Å for furan) of the free heteroarenes. The C(12)-C(13) bond (1.390(12) and 1.403(4) Å for **2** and **3**, respectively), on



the other hand, is significantly shorter than a single C-C bond, and the same bond (1.442(2)Å for thiophene, 1.4303(19)Å for furan) in the free heteroarene, indicating more electron delocalization in the ring. For all three complexes, the bond angles of the thienyl or furyl rings differ from the angles in uncoordinated thiophene and furan (Table 2.8), indicating ring involvement in stabilizing the carbene carbon.

**Table 2.10** Selected torsion angles of **2**, **3** and **5**

Bond	Torsion Angle (°)	
	<b>2</b> (Y = S)	<b>3</b> (Y = O)
C(6)-Mn(2)-C(10)-O(10)	45.5(10)	139.0(2)
C(7)-Mn(2)-C(10)-O(10)	135.1(10)	48.7(2)
Mn(2)-C(10)-C(11)-Y	171.0(10)	174.4(2)
Mn(2)-C(10)-C(11)-C(12)	-6.4(11)	173.3(3)
C(3)-Mn(1)-Mn(2)-C(6)	-46.0(3)	45.97(10)
Bond	Torsion Angle (°)	
	<b>5</b>	
C(4)-Re(1)-C(10)-O(10)	3.5(4)	
C(2)-Re(1)-C(10)-O(10)	177.7(3)	
Re(1)-C(10)-C(11)-O(11)	-5.4(5)	
Re(1)-C(10)-C(11)-C(12)	175.6(4)	
Re(2)-Re(1)-C(10)-C(11)	-87.2(3)	
C(3)-Re(1)-Re(2)-C(8)	-30.93(19)	

The staggered conformation of the carbonyls are shown by the dihedral angle C(3)-Mn(1)-Mn(2)-C(6) of -46.0(3)° for **2**, and 45.97(10)° for **3** (Table 2.10). The rhenium complex shows a smaller dihedral angle (C(3)-Re(1)-Re(2)-C(8) - 30.93(19)°) which indicates a less symmetric staggered conformation, due to the longer Re-Re bond length.

For complex **5**, the Re(1)-Re(2) bond distance (3.0809(3)Å) is longer than the Re-Re bond (3.0413(11)Å) reported for  $\text{Re}_2(\text{CO})_{10}$ <sup>[39]</sup> and is considerably longer than the Mn-Mn bond distance of **2** and **3** by approximately 0.15 Å. The bulky carbene ligand can therefore be accommodated in the equatorial position. Most  $\text{eq}[\text{Mn}_2(\text{CO})_9(\text{carbene})]$  complexes studied crystallographically have cyclic carbene ligands that display less steric hindrance compared to carbene complexes with two separate substituents<sup>[40;41]</sup>.

## 2.4 Conclusions

This study indicated that there may still be a lot to be discovered in the area of carbene complexes of manganese and rhenium; an area that has been neglected. The bulkiness of an  $\text{Mn}(\text{CO})_5$ -fragment can affect the coordination site of a carbene ligand. It is clear that although the equatorial position is the electronically favoured position for the carbene ligand, steric effects can force the carbene ligand to occupy an axial position. It was assumed that the carbene would have taken up an equatorial position based on the many reported studies of cyclic carbene ligands which are not very bulky<sup>[40-45]</sup>. The steric constraints are much more pronounced for the manganese complexes compared to the rhenium complexes, because of the much shorter Mn-Mn bond length compared to the Re-Re bond length. Complex **5** has its carbene ligand in the electronically favourable equatorial position.

It is possible to use infrared spectra to deduce the site of coordination of the carbene ligand, provided the spectra are carefully examined and possible band overlap is taken into account. This is useful if X-ray crystallography cannot be utilized for structure elucidation.

The possible manipulation of the position of the carbene ligand is planned in future work. This could be attempted by substitution of carbonyl ligands with bulky phosphine ligands<sup>[46]</sup>, known to substitute axially, to force the carbene ligand to adopt an equatorial position for the dimanganese complexes.

## 2.5 References

1. E.O. Fischer, A. Maasböl, *Angew. Chem. Int. Ed. Engl.* 3, **1964**, 645.
2. O.S. Mills, A.D. Redhouse, *J. Chem. Soc. A*, **1968**, 642.
3. E.O. Fischer, *Angew. Chem.* 86, **1974**, 651.
4. F.A. Cotton, C.M. Lukehart, *Prog. Inorg. Chem.* 16, **1972**, 487.
5. C.P. Casey, T.J. Burkhardt, *J. Am. Chem. Soc.* 95, **1973**, 5833.
6. J.A. Connor, E.M. Jones, *J. Chem. Soc. A*, **1971**, 1974.
7. W.A. Hermann, *Kontakte* 3, **1991**, 29.
8. S. Maiorana, A. Papagni, E. Licandro, A. Persoons, K. Clay, S. Houbrechts, W. Porzio, *Gazz. Chim. Ital.* 125, **1995**, 377.
9. M.M. Moeng, *Terthienyl Carbene Complexes*, University of Pretoria, **2001**.
10. A.J. Olivier, *Novel Carbene Complexes with Pyrrole Ligands*, University of Pretoria, **2001**.
11. C. Crause, *Synthesis and Application of Carbene Complexes with Heteroaromatic Substituents*, University of Pretoria, **2004**.
12. M. Landman, *Synthesis of Metal Complexes with Thiophene Ligands*, University of Pretoria, **2000**.
13. E.O. Fischer, E. Offhaus, *Chem. Ber.* 102, **1969**, 2449.
14. G. Huttner, D. Regler, *Chem. Ber.* 105, **1972**, 1230.
15. M.A. Schwindt, T. Lejon, L.S. Hegedus, *Organometallics* 9, **1990**, 2814.
16. M.F. Semmelhack, G.R. Lee, *Organometallics* 6, **1987**, 1839.
17. A. Rabier, N. Lugan, R. Mathieu, *J. Organomet. Chem.* 617-618, **2001**, 681.
18. C.P. Casey, S. Kraft, D.R. Powell, M. Kavana, *J. Organomet. Chem.* 617-618, **2001**, 723.
19. E.O. Fischer, P. Rustemeyer, *J. Organomet. Chem.* 225, **1982**, 265.
20. U. Schubert, K. Ackermann, P. Rustemeyer, *J. Organomet. Chem.* 231, **1982**, 323.

21. C.P. Casey, C.R. Cyr, R.L. Anderson, D.F. Marten, *J. Am. Chem. Soc.* 97, **1975**, 3053.
22. C.P. Casey, R.L. Anderson, *J. Am. Chem. Soc.* 93, **1971**, 3554.
23. C.P. Casey, C.R. Cyr, *J. Organomet. Chem.* 37, **1973**, C69.
24. R.J. Abrahams, J. Fischer, P. Loftus, *Introduction to NMR Spectroscopy*, John Wiley and Sons, **1988**.
25. E. Pretch, J. Seibl, T. Clerc, W. Simon, *Tables for Spectral Data for Structure Determination of Organic Compounds*, 2nd Ed. Springer-Verlag, Berlin/Heidelberg **1989**.
26. R.J. Cushley, R.J. Sykes, C.-K. Shaw, H.H. Wasserman, *Can. J. Chem.* 53, **1975**, 148.
27. S. Gronowitz, *Adv. Heterocycl. Chem.* 1, **1963**, 1.
28. B.A. Anderson, W.D. Wulff, A. Rahm, *J. Am. Chem. Soc.* 115, **1993**, 4602.
29. E.O. Fischer, T. Selmayr, F.R. Kreissl, U. Schubert, *Chem. Ber.* 110, **1977**, 574.
30. B.E. Mann, *Adv. Organomet. Chem.* 12, **1974**, 135.
31. Y.M. Terblans, H.M. Roos, S. Lotz, *J. Organomet. Chem.* 566, **1998**, 133.
32. P.S. Braterman, *Metal Carbonyl Spectra*, Academic Press Inc., London **1975**.
33. M.L. Ziegler, H. Haas, R.K. Sheline, *Chem. Ber.* 98, **1965**, 2454.
34. J.Fr. Janik, E.N. Duesler, R.T. Paine, *J. Organomet. Chem.* 323, **1987**, 149.
35. L.J. Farrugia, *J. Appl. Crystallogr.* 30, **1997**, 565.
36. The POV-Ray Team, POV-Ray **2004**, URL: <http://www.povray.org/download/>.
37. W.R. Harshbarger, S.H. Bauer, *Acta Crystallogr.* B26, **1970**, 1010.
38. P.B. Liecheski, D.W.H. Rankin, *J. Mol. Struct.* 196, **1989**, 1.
39. M.R. Churchill, K.N. Amoh, H.J. Wasserman, *Inorg. Chem.* 20, **1981**, 1609.
40. J.-A.M. Garner, A. Irving, J.R. Moss, *Organometallics*, 9, **1990**, 2836.
41. J.-A.M. Anderson, S.J. Archer, J.R. Moss, M.L. Niven, *Inorg. Chim. Acta* 206, **1993**, 187.

42. P.J. Fraser, W.R. Roper, F.G.A. Stone, *J. Chem. Soc., Dalton Trans.* **1974**, 760.
43. C.H. Game, M. Green, J.R. Moss, F.G.A. Stone, *J. Chem. Soc., Dalton Trans.* **1974**, 351.
44. C.H. Game, M. Green, F.G.A. Stone, *J. Chem. Soc., Dalton Trans.* **1975**, 2280.
45. D.H. Bowen, M. Green, D.M. Grove, J.R. Moss, F.G.A. Stone, *J. Chem. Soc., Dalton Trans.* **1974**, 1189.
46. N.J. Coville, A.M. Stolzenberg, E. L. Muetterties, *J. Am. Chem. Soc.* **1983**, 105, 2499.